Heliyon 8 (2022) e10275

Contents lists available at ScienceDirect

Heliyon

journal homepage: www.cell.com/heliyon

Research article

Removal of lead and chromium from solution by organic peels: effect of particle size and bio-adsorbent

Jeasson Steven Castañeda-Figueredo *, Ana Isabel Torralba-Dotor, Cristian Camilo Pérez-Rodríguez, Ana María Moreno-Bedoya, Carmen Stella Mosquera-Vivas **

Environmental Engineering, Faculty of Engineering, Universidad ECCI, 111311, Bogotá D.C, Colombia

ARTICLE INFO

Keywords:
Bio-adsorption
Orange
Potato
Passion fruit
Isotherms
Metals

ABSTRACT

A variety of organic wastes can be used in innovative methods to treat water pollution through the adsorption process. In this work, we evaluated the effect of particle size (500–2000, 250–500, and less than 250 μm) and bio-adsorbent (orange, potato, and passion fruit peels) on the removal of lead and chromium from solution. The size and type of peels affected the capacity to adsorb metal ions ($p < 0.05$). Passion fruit peel had the highest metal adsorption, followed by orange and potato, since the cation exchange capacity (217.70 ± 39.57 cmol (+) kg^{-1}) and the specific surface area (141.10–1095.29 cm^2 g^{-1}) were higher in the passion fruit rind. The size of the adsorbent did not affect the organic matter, ash, exchange capacity, surface chemistry, or pH of the peels. However, these properties differed among the bio-adsorbents ($p < 0.05$). The Freundlich equation explained the adsorption of the metallic ions on the orange rind and of lead on the passion fruit. The linear model was the best fit for the adsorption isotherms of the metals on potato peel. The adsorption of chromium on the passion fruit had a maximum adsorption capacity of 3.3 mg g^{-1}. These results indicate that plant waste materials, especially passion fruit peel, have the potential as feasible and low-cost adsorbents in pilot studies for the treatment of polluted water.

1. Introduction

The increase in the consumption of fruits and vegetables in recent years has led to higher amounts of agricultural production and plant waste. *Citrus* production worldwide is estimated at 89 million tons, with 15×10^6 tons of waste per year [1]. According to Locatelli et al. [2], the vast majority of the harvests of these fruits are used for industrial processing, and between 50 % and 75 % of the total weight of the fruit is considered by-product or waste. Passion fruit is produced mainly in countries of the Andean Region and is exported to obtain juices and pulps. In 2018, approximately 37,000 tons of passion fruit were produced, and industrial processing generated 90 % of the shell and seed waste [3]. Potato has one of the largest crop productions worldwide at more than 300 million tons [4]. During the industrial processing of potatoes, 70 to 140 million tons of peel waste are produced per year [5]. The generation of large quantities of wastes of plant origin [6] as the result of the industrialization and commercialization of products for human development and promotion of the world's economy has motivated the use and incorporation of waste into many economic value chains. Fruit and vegetable wastes are used for the extraction of bioactive compounds, production of enzymes and exopolysaccharides, synthesis of bioplastics and biopolymers, production of biofuels and charcoal, and use as bio-adsorbents for the removal of pollutants from solution [7, 8, 9, 10].

Bio-adsorbents obtained from plant wastes are considered a low-cost and easy-to-acquire alternative for water treatment systems that contain metals [8]. Metals are found naturally in the air, water, and soil due to volcanic eruptions, dust, marine aerosols, forest fires, and parent material or rock emergence [11]. However, metal concentrations may increase in the different environmental compartments due to use in industry, agriculture, combustion of coal or other fuels, mining, and domestic and industrial effluents [11, 12, 13]. Some metals bioaccumulate and biomagnify through the trophic chain [13]; which makes them a potential risk to the health of the human population and to ecosystems. For example, lead is a toxic substance that accumulates in living organisms and is associated with neurological, kidney, heart, immunological, carcinogenic, respiratory, and gastrointestinal diseases in humans [14,

* Corresponding author.
** Corresponding author.
E-mail addresses: stevencafi74@gmail.com (J.S. Castañeda-Figueredo), cmosquerav@ecci.edu.co (C.S. Mosquera-Vivas).

https://doi.org/10.1016/j.heliyon.2022.e10275
Received 26 April 2022; Received in revised form 27 June 2022; Accepted 9 August 2022

15]. Waste products from melon, potato, cucumber, peanuts, almonds, walnut, hazelnut, pistachio, tea, coconut, rice, and orange, among others [8, 9], have been explored as metal bio-adsorbents and are proposed as alternatives for the removal of metals [8]. Table 1 summarizes previous studies of the adsorption capacity of Cr (III), Cr (VI), and Pb (II) on orange, potato, and passion fruit peels and the effect of some properties of the bio-adsorbent on the removal of the metals from the solution. In general terms, the pH controls the adsorption capacity of the metals on the bio-adsorbents, and Pb (II) has the greatest retention and affinity on plant waste materials.

The review summarized in Table 1 evidences the need to establish the effect of particle size and bio-adsorbent on metal retention under similar conditions. Therefore, the objectives of this work are: i) to establish whether the particle size of the bio-adsorbent affects its characteristics and capacity to adsorb the metals Cr (III) and Pb (II) from solution, and ii) to compare the retention and affinity of Cr (III) and Pb (II) on bio-adsorbents of orange, potato, and passion fruit peels under laboratory conditions with a single adsorption assay. The results of this research will allow us to choose the best bio-adsorbents for further works about bio-stability and reusability of materials under dynamic conditions.

Table 1. Removal of Cr (III), Cr (IV) and Pb (II) by orange, potato, and passion fruit peels.

Bio-adsorbent	Treatment	Metals	The capacity for removal or adsorption	Effect of the properties of the bio-adsorbent on retention	Reference
Orange peel	Washed with tap water, three times with distilled water, drying at 80 °C and sieved (particles smaller than 150 μm).	Cr	The maximum adsorption capacity was 7.14 mg g^{-1}.	97% of metal is removed with 1.12 g of bio-adsorbent, pH 2, and at a temperature of 34.17 °C.	Ben Khalifa et al., 2019
Orange peel	Washed with distilled water and detergent, cut into 5.5 cm pieces, dried at 110 °C, grounded, and sieved (particles between 0.074 mm). The skins were treated at 250 °C, 350 °C, and 450 °C through pyrolysis.	Cd, Al, Cu, Ni, Zn, and Pb	In all the materials, there was a higher removal of Pb and lower retention of Al (Pb > Cu > Ni > Cd > Zn > Al). The maximum adsorption capacity of Pb (II) was 50.5 mg g^{-1}.	The metal absorption capacity was higher for the materials that were treated at 450 °C and at a pH of 2.00.	Santos et al., 2015.
Orange peel	Cut into small pieces, washed with distilled water, dried at 60 °C, ground, and sieved (particles smaller than 45 mm). The skin was modified with NaOH and $CaCl_2$ solutions at a concentration of 0.8M.	Cu, Pb, and Zn.	The maximum adsorption capacities for Cu (II), Pb (II), and Zn (II) on the modified skin were 70.73, 209.8, and 56.18 mg g^{-1}, respectively.	The treatment of the skin reduced the soluble organic matter in the effluents and increased the elimination rate of Pb (II) at a pH of 5.5; 2 h contact time; a temperature of 298 K and a bio-adsorbent: solution ratio of 0.10:25.	Feng and Guo, 2012.
Orange peel	Washed twice with distilled water, dried at 70 °C, and ground. Modified using solutions of NaOH (1%) and NaOH (4M) and CS_2.	Cu, Cd, Pb, Zn, and Ni.	The maximum adsorption capacities for Cu (II), Cd (II), Pb (II), Zn (II), and Ni (II) were 77.60, 76.75, 218.34, 49.85, and 15.45 mg g^{-1}, respectively.	Between 80% and 100% of most of the metal ions were adsorbed under weakly acidic conditions. The optimum pH range for adsorption tests was between 5 and 5.5, and Pb (II) had a stronger adsorption affinity using modified peels at a temperature of 25 °C.	Liang et al., 2010.
Orange peel	Washed with water, dried in the sun for 5–7 days, cut into small pieces, ground, and sieved (particles between 200 and 400 μm).	Pb	The maximum adsorption of Pb (II) on the orange peel was 19.146 mg g^{-1}.	The percentage of Pb (II) removal was 95.73% with a metal concentration of 80 ppm, a quantity of bio-adsorbent of 1.0 g, and a maximum pH of 2.00.	Jena and Sahoo, 2017 [59].
Potato peel	Washed with distilled water and 0.1M HCl. Dried at 103–110 °C overnight. Grounded and sieved (75 μm particles).	Cr	The maximum adsorption of Cr (VI) on potato peel was 3.28 mg g^{-1}. Due to the functional groups present in the potato peel there was limited adsorption of the metal.	The final elimination percentage for an initial concentration of Cr (VI) at 120 mg L^{-1} was 74.84%. Initial concentrations of 100 and 60 mg L^{-1} had elimination percentages of 87.79 and 93.31%, respectively.	Chen et al., 2014.
Potato peel	Washed with distilled water and dried at 100 °C overnight. Ground and sieved (particle size 0.45–0.15 mm).	Pb	The maximum adsorption of Pb (II) on potato peel was 217 mg g^{-1} at 20 °C.	At low initial concentrations, the Pb (II) was completely adsorbed onto the material, but at initial concentrations greater than 300 mg L^{-1}, the amount of non-adsorbed ions increased due to the saturation of the bio-adsorbent.	Kyzas and Mitropoulos, 2018
Passion fruit peel	Washed with distilled water and dried at room temperature until constant moisture, then placed in a water bath at 50 °C for 48 h and oven-dried at 50 °C for 24 h. Ground and sieved (200 mesh).	Cu, Cd, Ni, and Pb	The maximum adsorption of Pb (II) on the passion fruit peel was 63.9 mg g^{-1} at a flow of 3.00 mL min^{-1} and 98.4 mg g^{-1} at a pH = 6.0.	In a dynamic medium (columns) the adsorption of metals was affected by the flow rate and pH. The maximum adsorption capacities of the metals are obtained at a pH between 5.0 and 6.0.	Chao et al., 2014.
Passion fruit peel	Washed with distilled water and air dried at 70 °C for 8 h. Ground and sieved (particle size less than 500 μm)	Cr and Pb	The maximum adsorption of Cr (III) and Pb (II) in the passion fruit peel was 85.1 mg g^{-1} and 151.6 mg g^{-1}, respectively.	The maximum adsorption of metals on the bio-adsorbent was obtained at a pH of 5.0.	Jacques et al., 2007.

2. Materials and methods

2.1. Metals

The lead and chromium used in the elimination studies were obtained from lead (II) nitrate and chromium (III) nitrate nonahydrate, both with a purity of 98%. The $Pb(NO_3)_2$ and $Cr(NO_3)_3.9H_2O$ were supplied by Merck (Darmstadt, Germany). Standard solutions of Lead (II) and chromium (III) at 1,000 g L^{-1} in 0.5M HNO_3 were purchased from AppliChem Panreac (Castellar del Vallès, Spain). These solutions were used to quantify metals in the test solutions.

2.2. Organic peels

The orange (*Citrus sinensis*) OP, potato (*Solanum tuberosum*) PP, and passion fruit (*Passiflora edulis*) PF peels were collected at the local market. The peels were washed with potable water, cut into small pieces, and dried at room temperature and 50 °C. Then, the dried peels were grounded and sieved to achieve particle sizes of 500–2000, 250–500, and less than 250 μm on a sieve shaker equipped with ASTM 10-, 35-, and 60-mesh sieves. The sieve method allows the measurement of the equivalent particle diameter [16]; in this case, the particle diameter is equal to the diameter of the diagonal mesh of the sieve.

2.3. Properties of bio-adsorbents

2.3.1. Organic matter, ash content, and cation exchange capacity

The organic matter (OM) and ash content of the orange, potato, and passion fruit peels with particle sizes of 500–2000, 250–500, and less than 250 μm were determined in triplicate with the ignition method [17]. Briefly, a quantity (0.5000–2.0000 g) of bio-adsorbent was dried at 105 °C for 24 h in crucibles. Then, the crucibles were weighed at room temperature, oxidized at 440 °C in a muffle furnace for 5 h, and weighed at room temperature.

The cation exchange capacity (CEC) of OP, PP, and PF with a particle size of 500–2000, 250–500, and less than 250 μm was obtained by ammonium exchange with NaCl. Between 0.5000 and 2.0000 g of peel was added to 40 mL of 1N CH_3COONH_4 at pH = 7.00. They were stored for 24 h, stirred for 3 h, and filtered with 60 mL of ammonium solution. The residues were washed with 50 mL of ethanol, and the NH_4^+ was exchanged with 50 mL of 10 % NaCl. Twenty milliliters of 37 % formaldehyde was added to the supernatants and then titrated with 0.2 N NaOH to quantify the cmol (+) kg^{-1} of each bio-adsorbent [18]. All experiments were performed in triplicate for each bio-adsorbent and were run with blanks as controls.

The effect of lignocellulose polymers on the retention of cations in the bio-adsorbents was evaluated from the CEC in modified peels of OP, PP, and PF with a particle size of 500–2000 μm. The orange, potato, and passion fruit rinds were modified with alkaline solutions of NaOH and KOH. Fifteen grams of OP and PP and 3.5 g of PF were stirred with 200 mL of 0.4 M NaOH or 0.4 M KOH for 6–24 h. Then, the suspension was filtered and the residue was washed with deionized water until reaching a neutral pH and dried at 105 °C until reaching constant weight. The CEC of the dried residue was determined as described above. In the alkaline extractions of the peels, the residue is enriched with cellulose and the filtrate contains hemicellulose and lignin [19, 20].

2.3.2. Surface chemistry with fourier transform infrared spectroscopy

Fourier transform infrared spectroscopy (FTIR) was recorded in the range of 400–4000 cm^{-1}, with a resolution of 4 cm^{-1}, using an Alpha Platinum ATR Bruker equipment (Massachusetts, USA) for OP, PP, PF, and ashes (particle size 500–2000, 250–500, and less than 250 μm), and the dried residues of the alkaline treatments.

2.3.3. pH and zero charge pH (pH_{ZC})

The H^+ ion concentration in the solution (pH) of orange, potato, and passion fruit peels with particle sizes 500–2000, 250–500, and less than 250 μm was measured in triplicate using the EPA method 9045D [21]. One gram of the skins was placed in 50-mL beakers, and 25 mL of deionized water was added. The water/rind suspension was stirred intermittently for 1 h at 20 ± 5 °C, and then the pH was measured with a hydrogen electrode.

The size of the bio-adsorbents did not significantly affect the pH of the solution ($p < 0.05$). Therefore, a particle size of 500–2000 μm was selected for the pH_{ZC} measurements. The pH_{ZC} is the aqueous concentration of H^+ ions in which the adsorbent has a net charge equal to zero. Between 0.0100-1.0000 g of bio-adsorbent with a particle size of 500–2000 μm was weighed into 30-mL amber flasks. Ten milliliters of a 0.1M NaCl solution was added, and the suspensions were stirred and stored for 0, 1, 2, 3, 4, and 5d (equilibrium time) at 22 ± 2 °C. After each equilibrium time, the pH was measured with a hydrogen electrode. Additionally, the pH_{ZC} of OP, PP, and PF was measured after 4d, 2d, and 2d of equilibrium, respectively, at 12 ± 2 °C and 32 ± 2 °C. All experiments were performed in triplicate for each type of peel, equilibrium time, and temperature, and were run with water blanks and 0.1M NaCl.

2.3.4. Textural properties with particle and bulk density

The particle density of OP, PP, and PF was evaluated in triplicate using the pycnometer method [18]. We weighed an aliquot of each bio-adsorbent with particle sizes 500–2000, 250–500, and less than 250 μm that had been dried at 105 °C in a pre-weighed pycnometer, added 2/3 of distilled water, and degassed at room temperature for 30 min. Then, the pycnometer was filled with water and weighed. The pycnometer was also weighed with distilled water only. The values of particle density were used to calculate the specific surface area according to Equation (1) [22]:

$$S = \frac{6^*\lambda^*m}{\rho_p{}^*d_p} \quad \text{(Equation 1)}$$

where S is the specific surface area ($cm^2\ g^{-1}$), λ is the shape factor (1 for PP and 3.6 for OP, PF) [23], m is the mass of particles (g), ρ_p is the particle density (g cm^3), and d_p is the equivalent diameter of the particles (cm g). Equation (1) is useful when the materials show high macro-porosity and release volatiles during N_2 isotherms.

The bulk density (ρ_b) of orange, potato, and passion fruit rinds was determined in triplicate using the cylinder method [24]. We weighed 5.00 mL of the dried OP, PP, and PF with particle sizes 500–2000, 250–500, and less than 250 μm. The values of ρ_p and ρ_b were used to estimate the total porosity (f_t) of each bio-adsorbent (Equation 2).

$$f_t = 1 - \left(\frac{\rho_b}{\rho_p}\right)^*100\% \quad \text{(Equation 2)}$$

2.3.5. Removal of lead and chromium from the aqueous solution

Tests of lead and chromium removal from the aqueous solution were carried out with: i) adsorption tests on OP, PP, and PF with particle sizes of 500–2000, 250–500, and less than 250 μm; and ii) adsorption isotherms in OP, PP, and PF with a particle size of 500–2000 μm at 22 °C. The adsorption isotherms were performed only for the 500–2000 μm particle size since the characteristics of the bio-adsorbent were not affected by particle size. Additionally, the 500–2000 μm particle size allowed adequate water flow in tests with small columns packed with the adsorbent material.

The adsorption test on orange, potato, and passion fruit peels with particle sizes of 500–2000, 250–500, and less than 250 μm was carried out using the Batch method [10, 25, 26] with modifications. Briefly, 2.0000 g (OP and PP) or 0.5000 g (PF) was placed in triplicate in a 250-mL Erlenmeyer flask, and an aliquot (50 mL) of a Pb (II) and Cr (III) (10 mg L^{-1}) solution was added to each flask. The suspension was stirred

for 1 h at 22 °C and filtered. Thirty milliliters of the filtrate was digested with 5 mL of concentrated HNO_3 at 70 °C to a volume of approximately 5 mL. The solution was kept at room temperature, then an additional 5 mL of concentrated HNO_3 was added and heated (70 °C) to a volume close to 5 mL. The previous step was performed one more time and the solution was diluted to 50 mL. A volume of the final solution was injected into an atomic absorption spectrometer (Contra AA 700 analitikjena. Konrad-Zuse-Strasse 1, Germany) to quantify the amount of lead and chromium in the solution at 283 nm and 357 nm, respectively. Metal recoveries were 97.57 ± 4.96% for Cr (III) and 98.10 ± 4.01% for Pb (II). The limits of detection (LOD) of the compounds were estimated at 0.55 mg L^{-1} for Cr (III) and 0.09 mg L^{-1} for Pb (II), and their limits of quantification (LOQ) were 1.66 mg L^{-1}, 0.27 mg L^{-1} for Cr (III) and Pb (II), respectively. The concentration range of Cr (III) (0.10–4.00 mg L^{-1}) and Pb (II) (0.10–2.00 mg L^{-1}) showed a linear regression, an intercept statistically equal to zero, and no deviation from linearity ($p < 0.05$).

The adsorption isotherms of OP, PP, and PF with a particle size of 500–2000 μm were carried out in a similar way to the adsorption tests. The initial concentration of the metals (Cr (III) and Pb (II)) ranged between 5.0 and 500.0 mg L^{-1} and all of the experiments were carried out in triplicate and performed with metal samples in solution; the blanks were the bio-adsorbents in water. According to the adsorption kinetics of chromium on OP, PP, and PF and of lead on OP and PF with a particle size of 500–2000 μm (Figure 1), instantaneous retention of Cr (III) and Pb (II) was observed in the bio-adsorbents at zero contact time. The 1-h equilibrium time showed maximum retention of Cr (III) in PF and in lead in OP and PF. Then, the adsorption of Cr (III) on PF and of Pb (II) on OP decreased slightly, and the adsorption of Pb (II) on PF remained constant over time. The absorbed amount of Cr (III) on PP and OP at 1 h was similar to that at zero contact time. Then, the adsorption of Cr (III) on PP and OP decreased over time. One hour was the equilibrium time selected for the adsorption tests and adsorption isotherms.

2.4. Data analysis

The adsorption isotherms of chromium and lead on OP, PP and PF were adjusted to the linearization of Hanes - Woolf (Equation 3), Lineweaver - Burk (Equation 4), Eadie - Hoffsiee (Equation 5), and Scatchard (Equation 6) from the Langmuir model (Equation 7); to the Freundlich model (Equation 8) and the linear model (Equation 9) [27, 28].

$$\frac{C_e}{q_e} = \left(\frac{1}{Q^{\circ}_{max}}\right) C_e + \frac{1}{Q^{\circ}_{max} K_L} \quad \text{(Equation 3)}$$

$$\frac{1}{q_e} = \left(\frac{1}{Q^{\circ}_{max} K_L}\right) \frac{1}{C_e} + \frac{1}{Q^{\circ}_{max}} \quad \text{(Equation 4)}$$

$$q_e = \left(\frac{-1}{K_L}\right) \frac{q_e}{C_e} + Q^{\circ}_{max} \quad \text{(Equation 5)}$$

$$\frac{q_e}{C_e} = -K_L q_e + Q^{\circ}_{max} K_L \quad \text{(Equation 6)}$$

$$q_e = \frac{Q^{\circ}_{max} K_L C_e}{1 + K_L C_e} \quad \text{(Equation 7)}$$

$$q_e = K_F C_e^n \quad \text{(Equation 8)}$$

$$q_e = K_D C_e \quad \text{(Equation 9)}$$

where C_e is the equilibrium concentration of metals in the solution (mg L^{-1}), q_e is the amount of metal adsorbed per unit of mass (mg kg^{-1}), Q°_{max} is the maximum saturated single-layer adsorption capacity of the bio-adsorbent (mg g^{-1}), K_L is a constant related to the affinity between the adsorbed metal and the bio-adsorbent (L mg^{-1}), K_F is the Freundlich

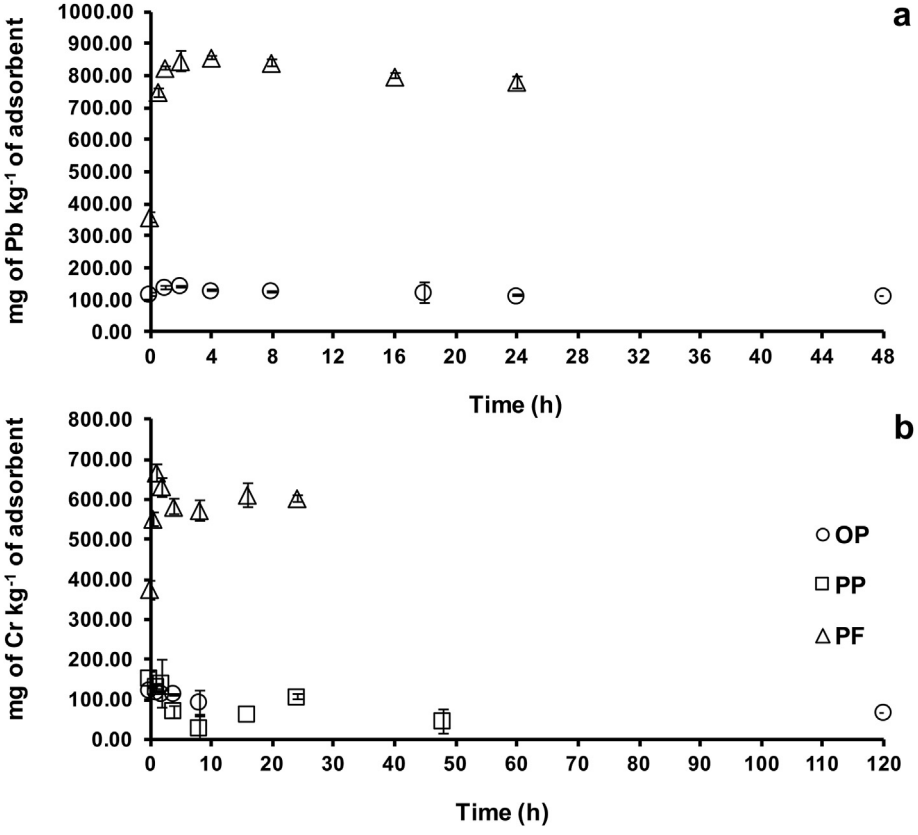

Figure 1. Metal adsorption kinetics of the bio-adsorbents. (a) Lead adsorption kinetics on orange (OP) and passion fruit (PF) peels. (b) Chromium adsorption kinetics on orange (OP), potato (PP), and passion fruit (PF) peels. Bars show the standard deviation of the mean.

Table 2. Properties of the bio-adsorbents of orange, potato, and passion fruit peels.

Peel	Size, μm	Organic Matter, %	Ash, %	The capacity of cationic exchange, cmol(+) kg^{-1}	pH	Particle density, g cm^{-3}	Bulk density, g cm^{-3}	Total porosity, %	Specific surface area, cm^2 g^{-1}
Orange (OP)	500–2000	95.63 ± 0.13	4.37 ± 0.13	146.02 ± 16.21	4.37 ± 0.12	1.55 ± 0.19	0.45 ± 0.001	71.16	121.01 ± 0.09*
	250–500	96.17 ± 0.34	3.83 ± 0.34	161.17 ± 12.81	4.44 ± 0.07	1.73 ± 0.48	0.45 ± 0.015	74.22	477.38 ± 0.35*
	<250	96.06 ± 0.40	3.94 ± 0.40	157.84 ± 4.53	4.25 ± 0.04	1.83 ± 0.09	0.46 ± 0.003	74.97	939.37 ± 0.69*
Potato (PP)	500–2000	93.26 ± 0.59	6.74 ± 0.59	60.33 ± 9.69	5.85 ± 0.18	1.86 ± 0.07	0.62 ± 0.002	48.08	31.84 ± 0.02*
	250–500	93.28 ± 0.15	6.72 ± 0.15	67.23 ± 3.76	6.18 ± 0.12	1.50 ± 0.27	0.58 ± 0.000	65.38	130.40 ± 0.29*
	<250	93.75 ± 0.30	6.25 ± 0.30	50.76 ± 9.03	6.14 ± 0.12	1.74 ± 0.18	0.67 ± 0.004	54.90	258.94 ± 0.44*
Passion fruit (PF)	500–2000	94.04 ± 0.12	5.96 ± 0.12	219.84 ± 22.24	4.89 ± 0.04	1.20 ± 0.11	0.40 ± 0.002	78.49	141.10 ± 0.10*
	250–500	93.89 ± 0.08	6.11 ± 0.08	195.54 ± 18.09	4.85 ± 0.01	1.69 ± 0.37	0.46 ± 0.000	69.60	556.62 ± 0.41*
	<250	92.35 ± 1.45	7.65 ± 1.45	237.74 ± 64.01	4.85 ± 0.04	1.49 ± 0.42	0.40 ± 0.004	76.84	1095.29 ± 0.80*

The ± sing is the standard deviation of the mean.

* The specific surface area of OP, PP, and PF was calculated based on the average of the particle density of each peel, since the particle size of the bio-adsorbent did not affect the particle density (OP: p = 0.544, PP: p = 0.149, and PF: p = 0.264).

adsorption affinity (mg kg^{-1}/(mg L^{-1})^n, where n is the adsorption energy (dimensionless) and K_D is the distribution coefficient (L kg^{-1}).

An ANOVA was performed to evaluate the effect of the particle size (500–2000, 250–500, and less than 250 μm) and of the bio-adsorbent type on organic matter, ash content, CEC, pH, and the adsorption capacity. All statistical analyses considered an alpha value of 0.05.

3. Results and discussion

3.1. Properties of the bio-adsorbent

3.1.1. Organic matter, ash content, cationic exchange capacity, FTIR, pH, and pH_{ZC}

The organic matter (OM), ash content, CEC, and pH of OP, PP, and PF with particle sizes of 500–2000, 250–500, and less than 250 μm are summarized in Table 2. The particle size of the bio-adsorbent did not affect the OM (OP: p = 0.162; PP: p = 0.291 and PF: p = 0.088), ash content (OP: p = 0.162; PP: p = 0.291 and PF: p = 0.088), CEC (OP: p = 0.346; PP: p = 0.111 and PF: p = 0.484), or pH (OP: p = 0.084; PP: p = 0.062 and PF: p = 0.317).

These properties did differ among the three bio-adsorbents ($p < 0.05$). The OP had the highest percentage of OM (95.95 ± 0.36%) and the lowest ash content (4.05 ± 0.36%). OM and ash content were statistically similar (p = 0.989) between PP and PF, with values of 93.43 ± 0.42% (OM), 6.57 ± 0.42% (ash) for PP and 93.43 ± 1.09% (OM), 6.57 ± 1.09% (ash) for PF. The OM values in the bio-adsorbents can be explained by the lignocellulose polymer, protein, starch, and pectin contents of the peels. According to the FTIR spectra of OP, PP, and PF for particle sizes of 500–2000, 250–500, and less than 250 μm (Figure 2 and Table 3); the vibration bands of the peels were similar at different sizes. The spectra of all of the bio-adsorbents showed a weak and broad band near 3282 cm^{-1} (O–H vibration due to intermolecular H bonds), two peaks at 2920 and 2852 cm^{-1} (aliphatic C–H vibration), one band from 1636 to 1603 cm^{-1} (conjugated and nonconjugated C = C stretch vibrations or absorbed

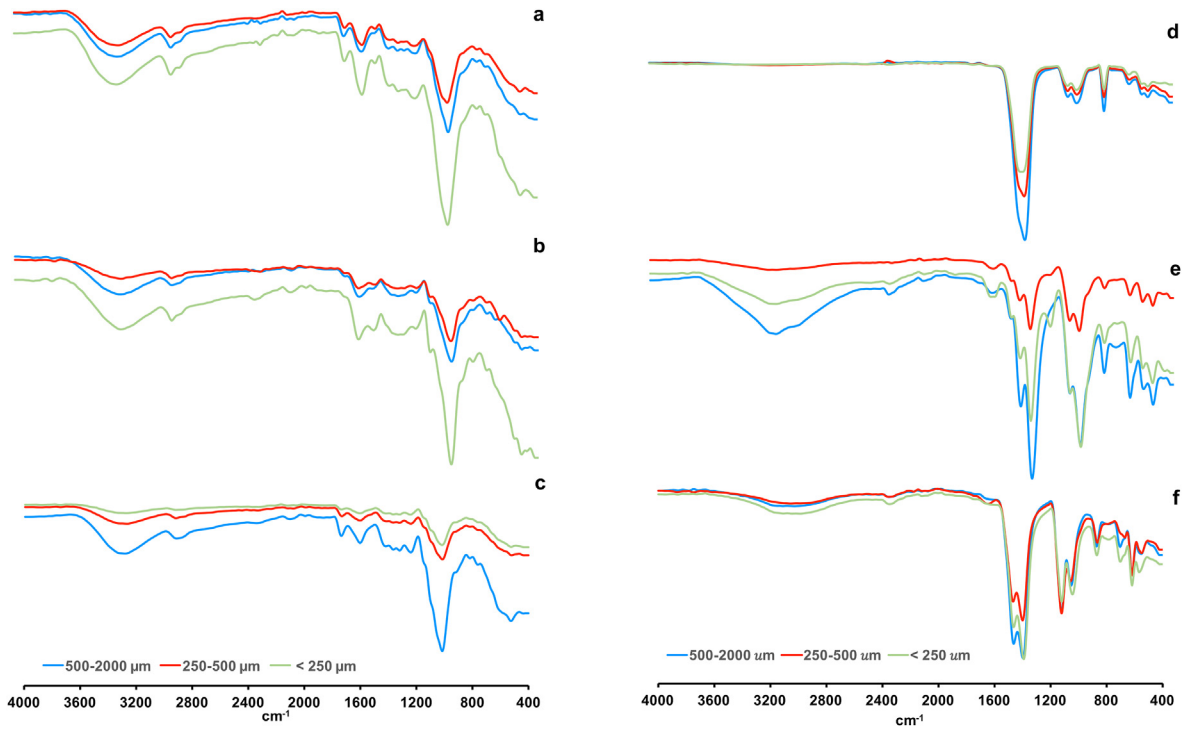

Figure 2. FTIR spectra of the bio-adsorbents and ash at different particle sizes. (a) FTIR spectra of orange (OP). (b) FTIR spectra of potato (PP). (c) FTIR spectra of passion fruit (PF). (d) FTIR spectra of orange ash. (e) FTIR spectra of potato ash. (f) FTIR spectra of passion fruit ash.

Table 3. Wave numbers of the FTIR bands of orange, potato, and passion fruit peels.

Orange FTIR, cm^{-1}	Potato FTIR, cm^{-1}	Passion fruit FTIR, cm^{-1}	Assignment
3290	3272	3283	ν(OH)
2920 2862	2919 2853	2913 2852	ν(CH)
1728	———	1736	ν(COOH)
1605	1636	1603	ν(C=C)
1358	1365	1365	δ(CH)
1017	999	1015	ν(CC) (CO)
Orange ash FTIR, cm^{-1}	Potato ash FTIR, cm^{-1}	Passion fruit FTIR, cm^{-1}	Assignment
1432	1450	1461	ν_3(C–O)
1121	1111	1119	ν_{as}(SO4)
1056	1044	1054	ν_{ss}(SO4)
873	876	867	ν_2(C–O)
700	696	668	ν_2 (C–O)
613	607	618	ν_4 (O–P–O)
572	540	550	ν_4 (O–P–O)

water in the biopolymers), peaks near 1362 cm^{-1} (bending on the C–H plane) and a strong band from 1017 to 999 cm^{-1} (C–O stretch of polysaccharides). The orange and passion fruit peels had a weak peak (1736 - 1728 cm^{-1}) that was assigned to the C=O stretch of COOH [29, 30, 31, 32]. The FTIR spectra confirm the complexity and diversity of the structural composition of all plant wastes. In general, carbohydrates (cellulose, soluble sugars, and hemicellulose), pectin, protein, and lignin explained the FTIR bands between 3300 and 999 cm^{-1} for OP and PF [33, 34]. Meanwhile, starch (amylose and amylopectin) was the predominant constituent of PP [33, 35].

The FTIR spectra of the ashes (Figure 2 and Table 3) indicated that the mineral fraction of the peels had characteristic bands of carbonate, sulfate, and phosphate compounds. These functional groups were verified with additional tests, including a comparison with FTIR spectra of salts with purity above 99%. A broad peak around 1418 cm^{-1} (OP = 1432 cm^{-1}; PP = 1450 cm^{-1}; PF = 1461 cm^{-1}) resulted from the C–O antisymmetric stretch vibration of the carbonate group. This type of compound also gave rise to the bands at 873 and 698 cm^{-1} (OP = 873 and 700 cm^{-1}; PP = 876 and 696 cm^{-1}; PF = 867 and 668 cm^{-1}) of bending vibrations. The presence of carbonate functional groups in the ashes was verified with an aqueous solution of HCl (10%). The ashes of orange, potato, and passion fruit all produced CO_2 (bubbles) in contact with the HCl. The bands appearing at 1121 cm^{-1} (OP), 1111 cm^{-1} (PP), and 1119 cm^{-1} (PF) were assigned to the asymmetric stretching of the sulfate groups (SO_4). SO_4 also resulted in the peaks at 1056 cm^{-1} (OP), 1044 cm^{-1} (PP), and 1054 cm^{-1} (PF) of symmetric stretching. The bands close to 600 and 559 cm^{-1} (OP = 613 cm^{-1}, 572 cm^{-1}; PP = 607 cm^{-1}, 540 cm^{-1}; PF = 618 cm^{-1}, 550 cm^{-1}) resulted from the O–P–O bending vibrations of the phosphate PO_4 groups. The presence of phosphate in the ashes was verified by colorimetric determination. The Bray I extract from the orange, potato, and passion fruit ashes produced a blue color with chloro-molybdic acid and tin chloride [36].

The PF had the highest CEC (217.70 ± 39.57 cmol (+) kg^{-1}), followed by the OP (155.01 ± 12.63 cmol (+) kg^{-1}) and PP (59.44 ± 9.93 cmol (+) kg^{-1}). The difference in the CEC may be explained by the amount of lignocellulose polymer in the peels. For example, the alkaline treatment (0.4M NaOH and KOH) led to a decrease in the CEC of 70.85 % in PF and 34.99 % on OP. Meanwhile, the CEC of PP treated with alkaline solutions did not show any decrease (59.26 ± 6.42 cmol (+) kg^{-1}). The FTIR spectra of the alkaline residues of OP, PP, and PF (Figure 3) showed bands similar to those of the FTIR spectra of the untreated peels because the residue obtained from the alkaline treatment is rich in cellulose. The characteristic bands of the cellulose polymer were: i) a broad band near

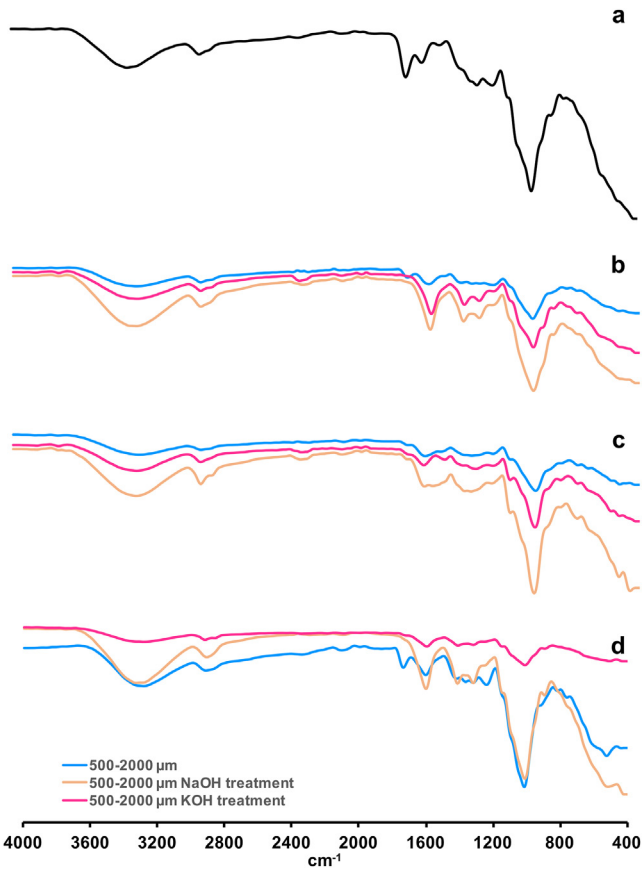

Figure 3. FTIR spectra of pectin and bio-adsorbent residues after alkaline treatments. (a) FTIR spectrum of passion fruit pectin. (b) FTIR spectra of the orange residues. (c) FTIR spectra of potato residues. (d) FTIR spectra of passion fruit residues.

3300 cm^{-1} (OP = 3303 cm^{-1} and PF = 3309 cm^{-1}) due to the O–H stretching vibration of inter and intramolecular hydrogen bonds in the cellulose; and ii) a broad band near 2900 cm^{-1} (OP = 2893 cm^{-1} and PF = 2905 cm^{-1}), attributed to the aliphatic C–H stretch vibration. In addition, there was a band from 1605 to 1603 cm^{-1} (vibration of water molecules absorbed in the biopolymer), a peak from 1434 to 1415 cm^{-1} (CH_2 in flexion C-6), a band from 1318 to 1316 cm^{-1} (CH_2 (wiggle) in flexion C-6), a peak from 1244 to 1242 cm^{-1} (C–OH on the plane in flexion C-6), and a strong band from 1016 to 983 cm^{-1} (C–O stretch of the polysaccharide) [37]. Passion fruit consists of ~80% (p/p) of non-starch polysaccharides, of which 42 % is cellulose, 25 % pectin, and 12 % hemicellulose [38]. The proximal composition of the orange peel shows 11 % cellulose and 21 % pectin, while potato peels are composed of ~67 % (p/p) starch polysaccharides [33]. According to this information, the PF bio-adsorbent had the highest amount of lignocellulose polymers; therefore, it showed the highest CEC. Furthermore, the dissociation of the carboxyl groups of the pectin in PF (vibrations close to 3300 cm^{-1}, OH; 1600 cm^{-1}, C = O (COO^-); and 1736 cm^{-1} C = O) were also responsible for adsorbing the cations in solution (Figure 3 (a)). The pectin was extracted from PF with 0.4M HNO_3 solution as previously mentioned in the alkaline extractions. The acidic extraction filtrate was used to obtain the pectin with absolute ethanol and record its FTIR spectrum (Figure 3 (a)).

The PP presented the highest pH value (6.05 ± 0.20), followed by the PF (4.86 ± 0.03) and the OP (4.35 ± 0.11). Additionally, these values were higher than the pH_{ZC} values (Figure 4 (a), (d), (g)) for OP (3.20–3.40 during 4 d), PP (4.80–4.90 during 2 d), and PF (3.80–3.90 during 2 d) at a particle size of 500–2000 µm and 22 °C. The values of pH > pH_{ZC} allow a net negative charge on the surface of the bio-adsorbents

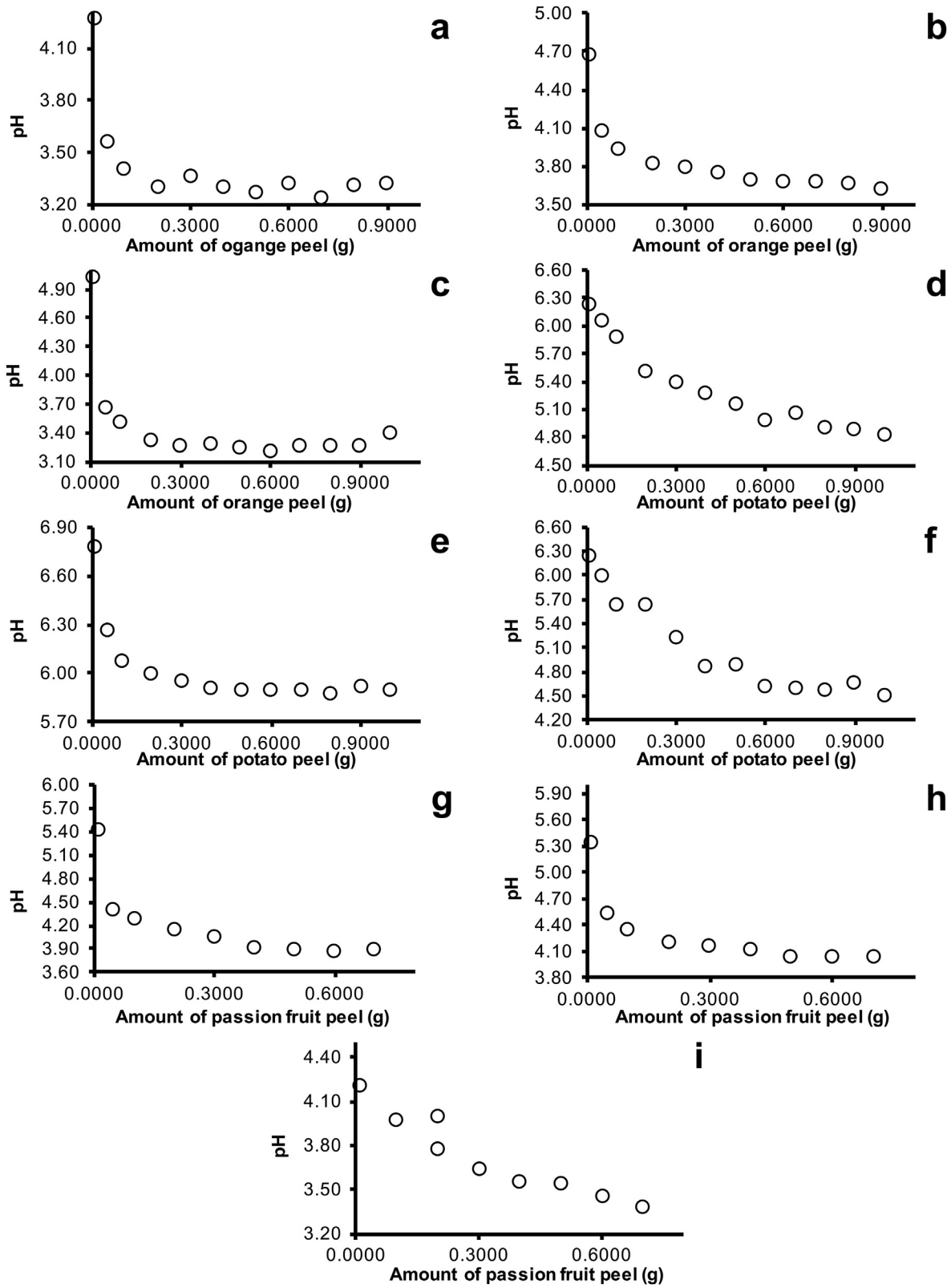

Figure 4. Zero charge pH (pH_{ZC}) of the bio-adsorbents at different temperatures. pH of orange peel at 22 °C (a), 12 °C (b), and 32 °C (c). pH of potato peel at 22 °C (d), 12 °C (e), and 32 °C (f). pH of passion fruit peel at 22 °C (g), 12 °C (h), and 32 °C (i).

[26, 39], due to the dissociation of the hydroxyl and carboxyl groups of the natural polysaccharides (pectin, hemicellulose, and lignin). This dissociation is also responsible for the pH values in the bio-adsorbents. The PP bio-adsorbent, which had the highest quantity of starch polysaccharides and the lowest quantity of lignocellulose polymers [33] showed the highest pH and pH_{ZC} values. The amount of cellulose, hemicellulose, lignin, and pectin in the orange and passion fruit peels [33, 38] allowed a higher concentration of H^+ ions in the aqueous solution. For example, the lignin-related phenols guaiacol and syringeal have pK_a values in water at 25 °C between 1.60 and 11.0 [40]. A low pK_a

value indicates that the substance is a strong acid and dissociates completely in water. Additionally, orange peels have acidic functional groups (carboxylic, lactone, and phenolic) on the surface [26].

The pH_{ZC} of the orange (3.60–3.70 for 4 d), potato (5.80–5.90 for 2 d), and passion fruit peels (4.00–4.01 for 2 d) increased and stabilized better with the decrease in temperature to 12 °C (Figures 4(b), (e), and (h)). Meanwhile, increasing the temperature to 32 °C did not affect the pH_{ZC} of the OP (Figure 4(c)) but decreased the pH_{ZC} of the PP (4.50–4.70 for 2 d) (Figure 4(f)) and the PF (3.30–3.50 for 2 d) (Figure 4(i)) due to microbial activity. For example, the fermentation of potato residues by thermophilic amylolytic microorganisms produces lactic acid [41], accompanied by a decrease in pH. Finally, the pH_{ZC} values of this study were lower than those published by Samarghandy et al. [42] for potatoes ($pH_{ZC} = 6.59$) and Gerola et al. [43] for passion fruit peel ($pH_{ZC} < 5.5$); and higher than those published by Ben Khalifa et al. [26] for orange peel ($pH_{ZC} = 2.5$).

3.1.2. Removal of lead and chromium from the aqueous solution

The amount of Cr (III) and Pb (II) in orange, potato, and passion fruit peels with particle sizes of 500–2000, 250–500, and less than 250 μm are summarized in Figure 5. Ben Khalifa et al. [26] found that a smaller particle diameter offers a greater metal removal efficiency for low amounts of bio-adsorbent (≤1 g) and that the adsorption percentage does not change significantly with particle size for greater amounts of adsorbent. However, in this study, the particle size of the bio-adsorbent affected the retention of lead and chromium in the three peels ($p < 0.05$), except for the adsorption of Cr (III) on PF ($p = 0.164$). The particle size 500–2000 μm adsorbed more chromium (222.55 ± 6.02 mg kg^{-1}) and lead (264.55 ± 1.46 mg kg^{-1}) in OP. In the case of the PP, the particle size 500–2000 μm retained more Cr (158.25 ± 3.39 mg kg^{-1}), but the lead was more adsorbed on the particle sizes of 250–500 and less than 250 μm (256.17 ± 2.17 mg kg^{-1}). Particle size less than 250 μm retained more lead (1077.47 ± 12.56 mg kg^{-1}) in PF.

The amount of Cr (III) and Pb (II) adsorbed differed among the bio-adsorbents ($p < 0.05$). PF had the highest metal adsorption, followed by OP and PP. In addition, the bio-adsorbents showed a higher affinity for lead (Figure 5), probably due to the speciation of the metal. According to the pH of the OP, PP, and PF (approximately 4–6), most of the lead exists as Pb (II) ions, and chromium is found as Cr (III), CrOH (II), and $Cr(OH)_2$ (I) [10, 44, 45]. Chromium ions increase four-fold in radius with hydration [46]; therefore, this metal was less retained in the orange, potato, and passion fruit peels. Several adsorbents have shown a better efficiency for lead retention than chromium [10]. The main mechanism for the adsorption of Cr (III) and Pb (II) in the OP, PP, and PF was the exchange of cations between the hydrogen ion present in the three bio-adsorbents and the metals, due to the decrease of the pH at the end of the adsorption tests (Figure 6). Furthermore, the net negative charge on the surface of the peels (pH values > pH_{ZC}) allowed an electrostatic attraction between the bio-adsorbents and the metals (Figure 6). The net negative charge (CEC) and the specific surface area explain the order of adsorption of Pb (II) and Cr (III) on the peels, since the CEC and the specific surface area (Table 2) were greatest in PF, followed by OP then by PP. The specific surface area of OP, PP, and PF increased with decreasing particle size (Table 2), but the values in this study were lower than those found by Amel et al. [47], Dey et al. [48], Feng and Guo [34], Kamsonlian et al. [49], Rosanti et al. [50], Salman and Ali [51] for orange peel (0.452–204 $m^2\ g^{-1}$), El-Azazy et al. [52] for potato rind (4.075 $m^2\ g^{-1}$), and Chen et al. [53] for passion fruit peel (4.403 $m^2\ g^{-1}$).

The effect of particle size on the adsorption of metallic ions is explained by the difference in the specific surface area, swell, and porosity of the bio-adsorbents. Although the specific surface area of orange peel increased with decreasing particle size (500–2000 μm: 121.01

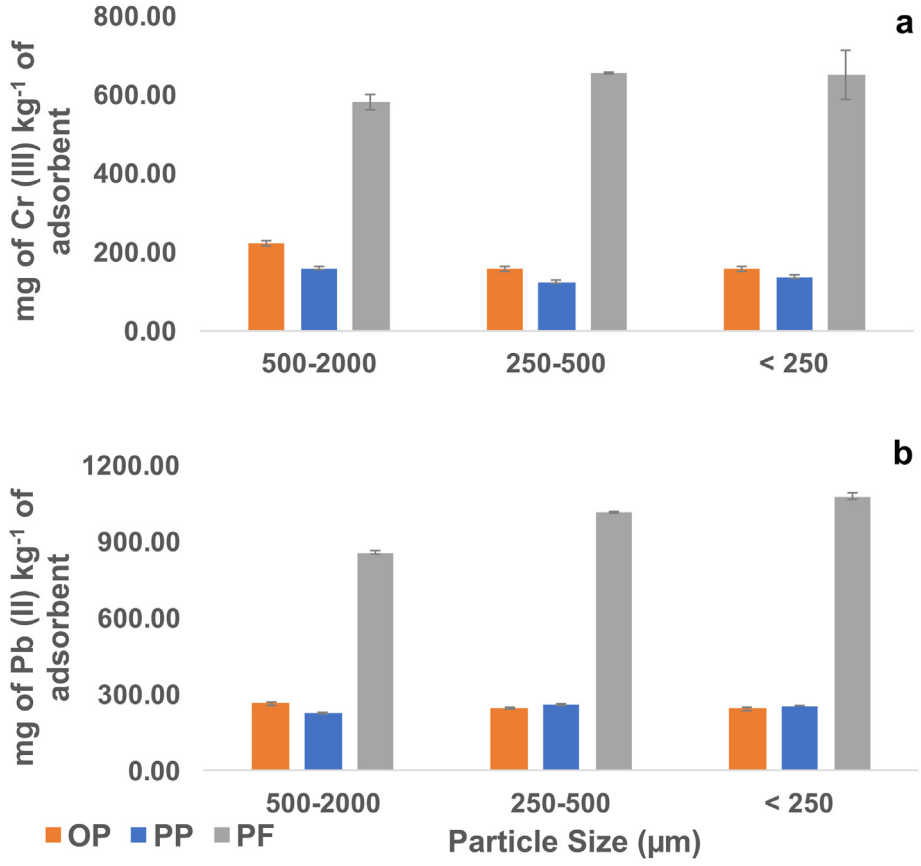

Figure 5. Metal adsorption on the bio-adsorbents at different particle sizes. Adsorption on orange (OP), potato (PP), and passion fruit (PF) peels of chromium (a) and lead (b). Bars show the standard deviation of the mean.

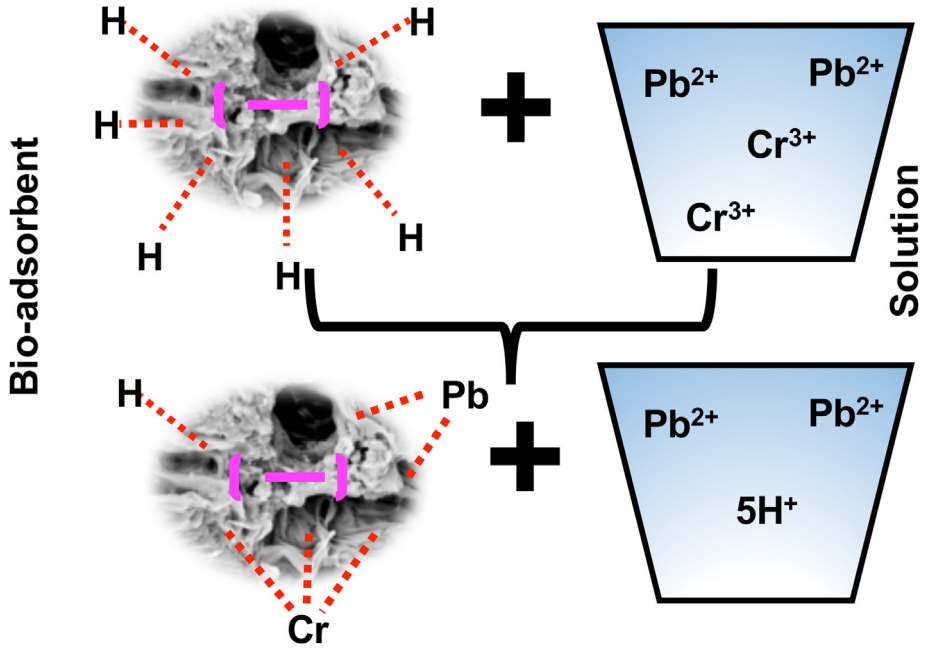

Figure 6. Schematic representation for removal of Pb (II) and Cr (III) from solution with the bio-adsorbents.

± 0.09 $cm^2\ g^{-1}$, 250–500 μm: 477.38 ± 0.35 $cm^2\ g^{-1}$, and less than 250 μm: 939.37 ± 0.69 $cm^2\ g^{-1}$), the Cr (III) and Pb (II) were adsorbed more on OP 500–2000 μm because particles between 250–500 μm and less than 250 μm were swelled in aqueous solution. This hydration increased particle density with decreasing particle size (Table 2) and could decrease the abundance of adsorption sites with adequate size for the retention of Cr (III). Pb (II) is adsorbed on the swelled bio-adsorbents between 250–500 μm (PP) and less than 250 μm (PF) because lead has a lower ionic radius than chromium. Furthermore, the PP between 250–500 μm and PF less than 250 μm had the highest porosity (65.38 %) and specific surface area (1095.29 ± 0.80 $cm^2\ g^{-1}$), respectively, among the bio-adsorbent particle size combination.

Table 4 summarizes the adsorption parameters (Q°_{max}, K_L, K_F, n, and K_D) and the coefficient of determination R^2 calculated to fit the experimental adsorption isotherms of Cr (III) and Pb (II) to the Hanes-Woolf, Lineweaver-Burk, Eadie-Hoffsiee, Scatchard, Freundlich and Linear equations. According to the R^2 values, the Freundlich model was a better fit to the adsorption isotherms of chromium and lead in the orange peel (R^2 = 0.991 and 0.972). The L-type isotherms ($n < 1$) show a strong interaction between the bio-adsorbent and the adsorbates, a strong influence of the initial concentration, and that the metals must be retained in some lower-energy sites, since the high-energy sites may have become saturated with the increase of the initial concentration [25]. The influence of the initial concentration was more marked in the adsorption of Cr (III) because the value of n was lower (Cr = 0.77 and Pb = 0.90). Additionally, the Freundlich adsorption affinity (K_F) of Cr (III) and Pb (II) were 136.39 and 321.24 (mg kg^{-1}/(mg L^{-1})^n, respectively. According to the K_F values, the orange peel showed a higher affinity for lead. In previous studies, several authors found that the retention of chromium and lead on the surface of the adsorbents was a better fit to single-layer adsorption (Langmuir model). The maximum saturated single-layer adsorption capacity was 7.1 mg g^{-1} for Cr (VI) and 14.64–218.34 mg g^{-1} for Pb (II) on the orange peel without and with modifications [26, 30, 34, 54], and of 250.0 mg g^{-1} for Cr (VI) on mousami (sweet lemon) peel [55].

The linear model had the best fit to the adsorption isotherms of chromium and lead on the potato peel (R^2 = 0.940 and 0.999). The linear equation over a wide concentration range indicated that all adsorption sites on the bio-adsorbent have equal energy to interact with the pollutants [25]. The occurrence of this type of isotherm in the potato peel can be explained by the morphology of the bio-adsorbent surface. Scanning electron micrographs show that PP surface is more homogeneous than the surface of the OP, which had an irregular and rough surface (Figure 5). The distribution coefficient (K_D) of Cr (III) and Pb (II) was 16.82 and 30.03 L kg^{-1}, respectively. Again, lead showed greater retention or affinity for the bio-adsorbent. Chen et al. [56], Kyzas and Mitropoulos [57] used the Langmuir and Freundlich models to explain the bio-adsorption of Cr (VI) on potato peel with Q°_{max}= 3.28 mg g^{-1} and K_F= 0.2985 (mg g^{-1}/mg L^{-1})^n, and the retention of Pb (II) on activated charcoal derived from potato peels with a Q°_{max}= 217 mg g^{-1} and K_F= 26.27 (mg g^{-1}/mg L^{-1})^n. The linear isotherm of the potato peel can be explained by the morphology of the bio-adsorbent surface. Scanning electron micrographs show that the PP surface is more homogeneous than the surface of the OP (Figure 7). The micrographs of potato peel at 450x showed similar spheres with a diameter range between 3 - 74 μm and pore space between 3 - 65 μm among the sizes. Meanwhile, the orange peel (micrographs at 450x) had an irregular and rough surface with pore space between 3 - 68 μm, 3–109 μm, and 4–44 μm for 500–2000 μm, 250–500 μm, and less than 250 μm, respectively. The irregular and rough surface and the pore space of the orange peel allowed higher adsorption of Pb (II) and Cr (III) than of potato peel.

The experimental adsorption isotherm of Cr (III) on the PF peel was best explained by the Hanes-Woolf equation (R^2 = 0.910), with a maximum saturated single-layer adsorption capacity (Q°_{max}) of 3.3 mg g^{-1} and a constant related to the affinity between the adsorbed metal and the bio-adsorbent (K_L) of 1.00 L mg^{-1}. The adsorption of Pb (II) was better fit by the Freundlich model (R^2 = 0.984) with a K_F= 927.64 (mg g^{-1}/mg L^{-1})^n and n= 0.55 (L-type isotherm). The homogeneity or heterogeneity of the bio-adsorbents can also be evaluated using the value of n. This parameter is related to the adsorption energies, and it has been established that the smaller the value of n, the greater the expected heterogeneity. When n= 1, the Freundlich equation reduces to a linear adsorption isotherm [28]. According to the value of n for Pb (II) in the PF, the surface of this bio-adsorbent had the greatest heterogeneity in adsorption energies. For both metals, it has been reported that the Langmuir equation best fit the adsorption isotherms with values of Q°_{max} of 85.1 mg g^{-1} for Cr (III) and 151.6 mg g^{-1} for the Pb (II) [58].

Table 4. Chromium and lead adsorption parameters on orange, potato, and passion fruit peels.

Rinds at 500–2000 μm	Adsorption parameters of chromium																
	Hanes-Woolf			Lineweaver-Burk			Eadie-Hoffsiee			Scatchard			Freundlich			Linear	
	Q°_{max} (mg g^{-1})	K_L (L mg^{-1})	R^2	K_L (L mg^{-1})	Q°_{max} (mg g^{-1})	R^2	K_L (L mg^{-1})	Q°_{max} (mg g^{-1})	R^2	K_L (L mg^{-1})	Q°_{max} (mg g^{-1})	R^2	K_F (mg kg^{-1}/mg $L^{-1})^n$	n	R^2	K_D L kg^{-1}	R^2
OP	12.5	0.008	0.968	0.012	10.0	0.981	0.013	9.0	0.760	-1.00×10^{-2}	110.20	0.760	136.39	0.77	0.991	31.15	0.983
PP	11.1	0.004	0.688	- 0.014	-2.0	0.978	0.018	4.0	0.144	-2.60×10^{-3}	42.52	0.144	43.96	0.91	0.939	16.82	0.940
PF	3.3	1.000	0.910	0.043	5.0	0.845	0.070	4.3	0.328	-2.70×10^{-2}	193.48	0.328	411.33	0.44	0.720	4.95	0.119
Rinds at 500–2000 μm	Adsorption parameters of lead																
	Hanes-Woolf			Lineweaver-Burk			Eadie-Hoffsiee			Scatchard			Freundlich			Linear	
	Q°_{max} (mg g^{-1})	K_L (L mg^{-1})	R^2	K_L (L mg^{-1})	Q°_{max} (mg g^{-1})	R^2	K_L (L mg^{-1})	Q°_{max} (mg g^{-1})	R^2	K_L (L mg^{-1})	Q°_{max} (mg g^{-1})	R^2	K_F (mg kg^{-1}/mg $L^{-1})^n$	n	R^2	K_D L kg^{-1}	R^2
OP	25.0	0.013	0.455	0.012	25.0	0.821	0.038	10.9	0.336	0.013	26.3	0.336	321.24	0.90	0.972	174.41	0.962
PP	12.5	0.005	0.497	0.053	2.0	0.988	0.018	5.4	0.395	0.007	10.5	0.395	99.93	0.75	0.990	30.03	0.999
PF	20.0	0.031	0.934	0.2504	5.0	0.939	0.079	13.8	0.630	0.050	17.9	0.630	927.64	0.55	0.984	59.37	0.935

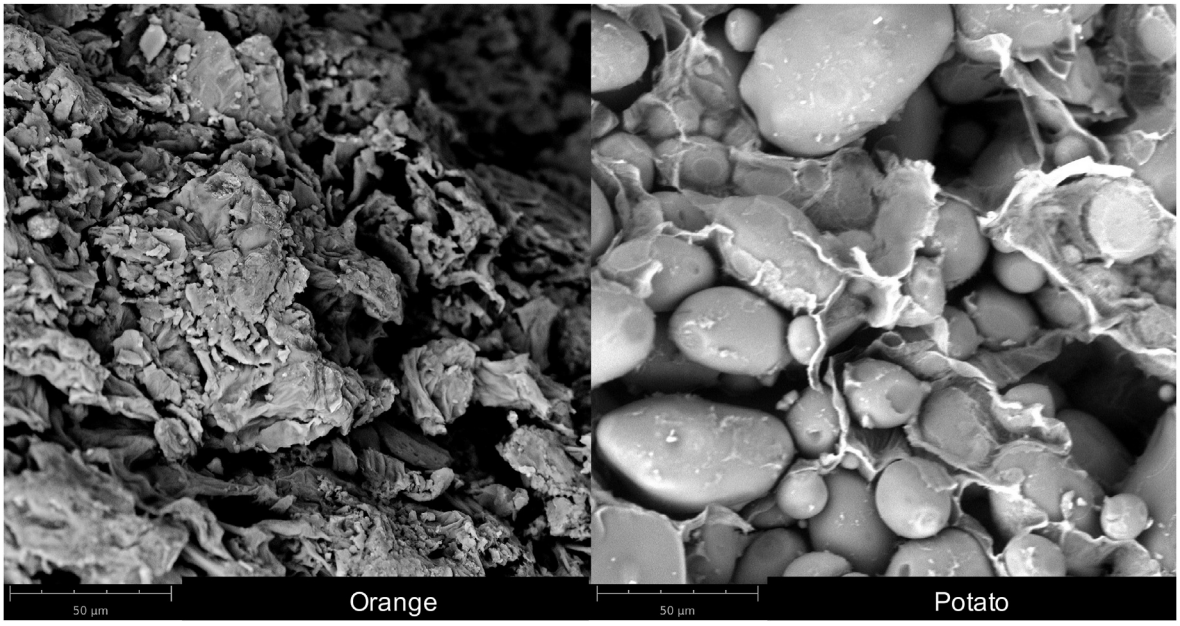

Figure 7. SEM (scanning electronic microscopy) micrographs of orange and potato peels.

Feng and Guo [34] reported that metal adsorption efficiencies increase when the pH of the solution increases from 2.5 to 6.0. At pH values above 6.0, the metallic ions precipitated due to the high hydroxyl concentrations in the aqueous solution. Therefore, the adsorption of chromium on OP (pH = 4.4) and PP (pH = 6.0), and of lead on OP (pH = 4.4) in this study were greater than those found by Ben Khalifa et al. [26], Santos et al. [30], Chen et al. [56] at pH between 2.0 - 2.5.

4. Conclusions

The objective of our research was to evaluate the effect of the particle size (500–2000, 250–500, and less than 250 μm) and of the bio-adsorbent (OP, PP, and PF) on the removal of lead and chromium from solution. We conclude that the particle size of the bio-adsorbent affects their adsorption of metallic ions; the 500–2000 μm particle size removed more Cr (III) and Pb (II) in most of the peels. The PF had higher metal ion adsorption due to its cationic exchange capacity and the specific surface area, and all of the peels showed a higher affinity for Pb (II). The Freundlich and linear models explained the adsorption isotherms of Cr (III) and Pb (II) on the orange and potato peels, respectively. The adsorption of metal ions on PF was explained by the Langmuir (chromium) and Freundlich (lead) models. The results obtained in this study indicate that plant wastes, especially from passion fruit, have potential as feasible and low-cost bio-adsorbent to remove metals from aqueous solutions.

Declarations

Author contribution statement

Jeasson Steven Castañeda-Figueredo & Ana Isabel Torralba-Dotor: Conceived and designed the experiments; Performed the experiments; Wrote the paper.

Cristian Camilo Pérez-Rodríguez & Ana María Moreno-Bedoya: Conceived and designed the experiments; Performed the experiments.

Carmen Stella Mosquera-Vivas: Conceived and designed the experiments; Performed the experiments; Analyzed and interpreted the data; Wrote the paper.

Funding statement

This research did not receive any specific grant from funding agencies in the public, commercial, or not-for-profit sectors.

Data availability statement

Data will be made available on request.

Declaration of interest's statement

The authors declare no conflict of interest.

Additional information

No additional information is available for this paper.

References

[1] N. M Hiri, I. Ioannou, M. Ghoul, N. Boudhrioua, Proximate chemical composition of orange peel and variation of phenols and antioxidant activity during convective air drying, J. New Sci. JS INAT 2015 (2015) 881–890.

[2] G. Locatelli, L. Finkler, C. Finkler, Orange and passion fruit wastes characterization, substrate hydrolysis and cell growth of cupriavidus necator, as proposal to converting of residues in high value-added product, An. Acad. Bras. Cienc. 91 (2019) 1–9.

[3] A. García-Reinoso, P. Areválo-Moscoso, Determinación de la capacidad de bioadsorción de metales pesados mediante el uso de la cáscara de maracuyá (Passiflora edulis) en aguas contaminadas, Master's thesis, Universidad Politécnica Salesiana, 2021.

[4] Faostat, Food and agriculture data (12th december 2017). http://www.fao.org/faostat/en/home.

[5] D. Wu, Recycle technology for potato peel waste processing: a review, Procedia Environ. Sci. 31 (2016) 103–107.

[6] B. Sellamuthu, V. Gandhi, B. Yadav, R. Tyagi, 21 - Sustainable production of bioadsorbents from municipal and industrial wastes in a circular bioeconomy context, in: A. Pandey, R.D. Tyagi, S. Varjani (Eds.), Biomass, Biofuels, Biochemicals, Elsevier, 2021, pp. 639–668.

[7] I. Esparza, N. Jiménez-Moreno, F. Bimbela, C. Ancín-Azpilicueta, L. Gandía, Fruit and vegetable waste management: conventional and emerging approaches, J. Environ. Manag. 265 (2020) 1105–1110.

[8] I. Anastopoulos, I. Pashalidis, A. Hosseini-Bandegharaei, D. Giannakoudakis, A. Robalds, M. Usman, L. Escudero, Y. Zhou, J. Colmenares, A. Núñez-Delgado, E. Lima, Agricultural biomass/waste as adsorbents for toxic metal decontamination of aqueous solutions, J. Mol. Liq. 295 (2019) 1–16.

[9] Y. Dai, Q. Sun, W. Wang, L. Lu, M. Liu, J. Li, S. Yang, Y. Sun, K. Zhang, J. Xu, W. Zheng, Z. Hu, Y. Yang, Y. Gao, Y. Chen, X. Zhang, F. Gao, Y. Zhang, Utilizations of agricultural waste as adsorbent for the removal of contaminants: a review, Chemosphere 211 (2018) 235–253.

[10] S. Pap, V. Bezanovic, J. Radonic, A. Babic, S. Saric, D. Adamovic, M. Turk Sekulic, Synthesis of highly-efficient functionalized biochars from fruit industry waste biomass for the removal of chromium and lead, J. Mol. Liq. 268 (2018) 315–325.

[11] P. Nagajyoti, K. Lee, T. Sreekanth, Heavy metals, occurrence and toxicity for plants: a review, Environ. Chem. Lett. 8 (2010) 199–216.

[12] H. Bart, B. Tangahu, S.S. Abdullah, H. Basri, M. Idris, N. Anuar, M. Mukhlisin, A review on heavy metals (as, pb, and hg) uptake by plants through phytoremediation, Int. J. Chem. Eng. 2011 (2011) 1–31.

[13] B. Montuelle, A. Steinman, R. Wuana, F. Okieimen, Heavy metals in contaminated soils: a review of sources, chemistry, risks and best available strategies for remediation, ISRN Ecology (2011) 1–20.

[14] ATSDR, Resúmenes de salud pública - plomo (lead) 6 de mayo de 2016, Acceded on 27th June 2021., 2016. Agencia para Sustancias Tóxicas y el Registro de Enfermedades, https://www.atsdr.cdc.gov/es/phs/es phs13.html.

[15] WHO, Lead poisoning and health (23th august 2019), Acceded on 27th June 2021., 2019. World Health Organization, https://www.who.int/news-room/fact-sh eets/detail/lead-poisoning-and- health.

[16] T.L. Eberhardt, S.-H. Min, Biosorbents prepared from wood particles treated with anionic polymer and iron salt: effect of particle size on phosphate adsorption, Bioresour. Technol. 99 (2008) 626–630.

[17] P. Rovira, V. Vallejo, Labile, recalcitrant, and inert organic matter in Mediterranean forest soils, Soil Biol. Biochem. 39 (2007) 202–215.

[18] IGAC, Capacidad de Intercambio Catiónico y Densidad de Partículas, IGAC 83–87, 2006, pp. 396–399.

[19] D. Yang, L.-X. Zhong, T.-Q. Yuan, X.-W. Peng, R.-C. Sun, Studies on the structural characterization of lignin, hemicelluloses and cellulose fractionated by ionic liquid followed by alkaline extraction from bamboo, Ind. Crop. Prod. 43 (2013) 141–149.

[20] H. Roghani-Mamaqani, N. Dinh Vu, H. Thi Tran, N. Bui, C. Duc Vu, H. Viet Nguyen, Lignin and cellulose extraction from vietnam's rice straw using ultrasound-assisted alkaline treatment method, Int. J. Polym. Sci. (2017) 1–8.

[21] US-EPA, Method 9045d: Soil and Waste Ph, United States Environmental Protection Agency, 2004.

[22] J. Wilkes, Fluid Mechanics for Chemical Engineers, Prentice-Hall, 1999.

[23] D.W. Green, M.Z. Southard, Perry's Chemical Engineers' Handbook, McGraw-Hill Education, New York, 2019. https://www.accessengineeringlibrary.com/content/book/9780071834087.

[24] U. Tiwari, E. Cummins, Chapter 7 - legume fiber characterization functionality, and process effects, in: B.K. Tiwari, Gowen, B. McKenna (Eds.), Pulse Foods, 2021, pp. 147–175.

[25] C. Mosquera-Vivas, M. Martínez, G. García-Santos, J. Guerrero-Dallos, Adsorption-desorption and hysteresis phenomenon of tebuconazole in Colombian agricultural soils: experimental assays and mathematical approaches, Chemosphere 190 (2018) 393–404.

[26] E. Ben Khalifa, B. Rzig, R. Chakroun, H. Nouagui, B. Hamrouni, Application of response surface methodology for chromium removal by ad- sorption on low-cost biosorbent, Chemometr. Intell. Lab. 189 (2019) 18–26.

[27] H. Tran, S.-J. You, A. Hosseini-BandegharaeI, H.-P. Chao, Mistakes and inconsistencies regarding adsorption of contaminants from aqueous solutions: a critical review, Water Res. 120 (2017) 88–116.

[28] S. Goldberg, Equations and Models Describing Adsorption Processes in Soils, John Wiley & Sons, 2005, pp. 489–517.

[29] C. Mosquera-Vivas, E. Hansen, G. García-Santos, N. Obregón-Neira, R. Celis-Ossa, C. González-Murillo, R. Juraske, S. Hellweg, J. Guerrero- Dallos, The effect of the soil properties on adsorption, single-point desorp- tion, and degradation of chlorpyrifos in two agricultural soil profiles from Colombia, Soil Sci. 181 (2016) 446–456.

[30] C. Santos, J. Dweck, R. Viotto, A. Rosa, L. De Morais, Application of orange peel waste in the production of solid bio-fuels and biosorbents, Bioresour. Technol. 196 (2015) 469–479.

[31] A. Synytsya, J. Čopíková, P. Matějka, V. Machovič, Fourier transform Raman and infrared spectroscopy of pectins, Carbohydr. Polym. 54 (2003) 97–106.

[32] C. Tejada-Tovar, A. González-Delgado, A. Villabona-Ortiz, Removal of Cr (VI) from aqueous solution using orange peel-based biosorbents, Indian J. Sci. Technol. 11 (2018) 1–13.

[33] A. Mahmood, J. Greenman, A. Scragg, Orange and potato peel extracts: analysis and use as bacillus substrates for the production of extracellular enzymes in continuous culture, Enzym. Microb. Technol. 22 (1998) 130–137.

[34] N.-C. Feng, X.-Y. Guo, Characterization of adsorptive capacity and mechanisms on adsorption of copper, lead and zinc by modified orange peel, T. Nonferr. Metal Soc. 22 (2012) 1224–1231.

[35] L. Amagliani, J. O'Regan, A. Kelly, J. O'Mahony, Chemistry, structure, functionality and applications of rice starch, J. Cereal. Sci. 70 (2016) 291–300.

[36] S. Dickman, R. Bray, Colorimetric determination of phosphate, Ind. Eng. Chem. Anal. Ed. 12 (1940) 665–668.

[37] V. Hospodarova, E. Singovszka, N. Stevulova, Characterization of cellulosic fibers by FTIR spectroscopy for their further implementation to building materials, Am. J. Anal. Chem. 9 (2018) 303–310.

[38] B. Yapo, K. Koffi, The polysaccharide composition of yellow passion fruit rind cell wall: chemical and macromolecular features of extracted pectins and hemicellulosic polysaccharides, J. Sci. Food Agric. 88 (2008) 2125–2133.

[39] S. Guiza, Biosorption of heavy metal from aqueous solution using cellulosic waste orange peel, Ecol. Eng. 99 (2017) 134–140.

[40] M. Ragnar, C. Lindgrend, N.-O. Nilvebrant, Appendix to the poster "on the dissociation constants of phenolic groups in lignin structures, in: Presented at the 10th International Symposium on Wood and Pulping Chemistry (ISWPC), 1999. Yokohama, Japan.

[41] M. Smerilli, M. Neureiter, S. Wurz, C. Haas, S. Frühauf, W. Fuchs, Direct fermentation of potato starch and potato residues to lactic acid by geobacil- lus stearothermophilus under non-sterile conditions, J. Chem. Technol. Biotechnol. 90 (2015) 648–657.

[42] M. Samarghandy, E. Hoseinzadeh, M. Taghavi, S. Hoseinazdeh, Biosorption of reactive black 5 from aqueous solution using acid-treated biomass from potato peel waste, Bioresources 6 (2011) 4840–4855.

[43] G. Gerola, N. Boas, J. Caetano, C. Tarley, A. Gonçalves, D. Dragunski, Utilization of passion fruit skin by-product as lead(II) ion biosorbent, Water, Air, Soil Pollut. 224 (2013) 1446.

[44] V. Gupta, I. Ali, T. Saleh, M. Siddiqui, S. Agarwal, Chromium removal from water by activated carbon developed from waste rubber tires, Environ. Sci. Pollut. Res. 20 (2013) 1261–1268.

[45] L. Overah, O. Ifeanyi, Evaluation of *dacryodes edulis* (native pear) seed biomass for Pb (II) sorption from aqueous solution, J. Appl. Sci. Environ. Manag. 21 (2017) 186–199.

[46] B. Conway, Ionic Hydration in Chemistry and Biophysics, Elsevier Scientific Publishing Company, 1981, pp. 1–774.

[47] K. Amel, I. Bendjamaa, T. Bensid, A. Meniai, D. Kerroum, Effect of calcination on orange peels characteristics: application of an industrial dye adsorption, Chem. Engineer. Trans. 38 (2014) 361–366.

[48] S. Dey, S. Basha, G. Babu, T. Nagendra, Characteristic and biosorption capacities of orange peels biosorbents for removal of ammonia and nitrate from contaminated water, Cleaner Materials 1 (2021), 100001.

[49] S. Kamsonlian, S. Sundaramurthy, C. Balomajumder, S. Chand, Characterization of banana and orange peels: biosorption mechanism, Int. J. Serv. Technol. Manag. 2 (2011) 1–7.

[50] A. Rosanti, Y. Kusumawati, F. Hidayat, A. Fadlan, A. Wardani, H. Anggraeni, Adsorption of methylene blue and methyl orange from aque- ous solution using orange peel and ctab-modified orange peel, Journal of the Turkish Chemical Society Section A: Chemistry 9 (2022) 237–246.

[51] T. Salman, M. Ali, Potential application of natural and modified orange peel as an eco–friendly adsorbent for methylene blue dye, Iraqi J. Sci. 57 (2016) 53.

[52] M. El-Azazy, A.S. El-Shafie, A.A. Issa, M. Al-Sulaiti, J. Al-Yafie, B. Shomar, K. Al-Saad, Potato peels as an adsorbent for heavy metals from aqueous solutions: eco-structuring of a green adsorbent operating Plackett-Burman design, J. Chem. (2019), 4926240.

[53] K. Chen, L. Du, P. Gao, J. Zheng, Y. Liu, H. Lin, Super and selective adsorption of cationic dyes onto carboxylate-modified passion fruit peel biosorbent, Front. Chem. 9 (2021).

[54] S. Liang, X.-Y. Guo, N.-C. Feng, Q.-H. Tian, Effective removal of heavy metals from aqueous solutions by orange peel xanthate, T. Nonferr. Metal Soc. 20 (2010) 187–191.

[55] R. Saha, K. Mukherjee, I. Saha, A. Ghosh, S. Ghosh, B. Saha, Removal of hexavalent chromium from water by adsorption on mosambi (*citrus limetta*) peel, Res. Chem. Intermed. 39 (2012) 2245–2257.

[56] Z.-S. Chen, F. Mutongo, O. Kuipa, P. Kuipa, Removal of cr (vi) from aqueous solutions using powder of potato peelings as a low-cost sorbent, Bioinorgan. Chem. Appl. (2014) 1–7.

[57] G. Kyzas, A. Mitropoulos, Zero-cost agricultural wastes as sources for activated carbons synthesis: lead ions removal from wastewaters, Proceedings 2 (2018).

[58] R. Jacques, E. Lima, S. Dias, A. Mazzocato, F. Pavan, Yellow passion-fruit shell as biosorbent to remove Cr(III) and Pb(II) from aqueous solution, Separ. Purif. Technol. 57 (2007) 193–198.

[59] S. Jena, R.K. Sahoo, Removal of Pb (II) from aqueous solution using fruits Peel as a low cost adsorbent, Int. J. Eng. Sci. Technol. 5 (1) (2017) 5–13.